THE LOW ENERGY BEAM TRANSFER (LEBT) LINE AND RFQ FOR THE MYRRHA PHASE 1 FACILITY

L. De Keukeleere, U. Dorda, J. Hustings, E. Tanke, J. Van De Walle, Belgian Nuclear Research Centre, Mol, Belgium

Abstract

At the Nuclear Research Center SCK CEN in Belgium, the first phase of the MYRRHA project (an accelerator driven system) is under construction. Included in MYRRHA Phase 1 are a normal-conducting injector linac followed by a superconducting linac, ultimately providing a CW proton beam of 4 mA and 100 MeV.

In this contribution, ongoing simulations of the Electron Cyclotron Resonance (ECR) ion source and Low Energy Beam Transfer (LEBT) line, which includes 2 solenoids, are described with an emphasis on the effects introduced by space charge and their effect on the performance. Details of the Radio Frequency Quadrupole (RFQ) simulations and benchmarking results as obtained with the codes Toutatis [1] and DYNAC [2] are presented.

INTRODUCTION

The MYRRHA (Multi-purpose hYbrid Research Reactor for High-tech Applications), currently under development at SCK CEN in Belgium, is a pioneering accelerator-driven system (ADS) designed for applications in nuclear waste transmutation, material research, and radioisotope production. A central component of this facility is a high-reliability proton accelerator delivering a continuous wave (CW) beam with strict requirements on beam losses and availability. To validate the accelerator concept and associated technologies, the first implementation phase, referred to as MYRRHA Phase 1, is presently under construction [3, 4].

The normal-conducting injector generates a high-intensity proton beam from an ECR ion source. This beam is subsequently transported through a LEBT line and injected into a Radio Frequency Quadrupole (RFQ), operating at 176.1 MHz. The RFQ bunches and accelerates the beam from 30 keV to 1.5 MeV. A schematic overview of the accelerator layout up to the RFQ is shown in Fig. 1. Downstream, CH cavities and a superconducting linac accelerate the beam to 100 MeV.

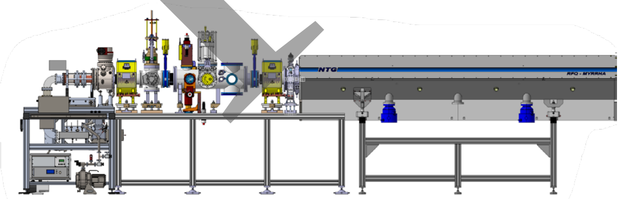

Figure 1: Layout of the injector front-end showing the ion source on the left side, the LEBT and, RFQ tank at a length of 4 m.

INJECTOR FRONT-END

The injector front-end, consisting of the ECR source, LEBT, and RFQ, determines beam quality and transmission. Space-charge effects are significant in the LEBT and require compensation.

Efficient RFQ operation relies on precise matching of the transverse phase space to its acceptance, as well as adequate longitudinal capture during the bunching process. While beam losses this stage should be minimized, accurate matching of the RFQ output is essential, as longitudinal tails may induce losses in the downstream linac.

Beam dynamics simulations are performed using TraceWin and DYNAC. TraceWin supports multi-particle tracking with space-charge modelling through field maps, and is coupled to the Toutatis package for RFQ simulations using time-based integration. DYNAC also provides multi-particle tracking with space-charge modelling, but uses the PARMTEQ/GENRFQ approach [5] for the RFQ. The comparison between these approaches enables benchmarking of the predicted beam dynamics.

RFQ ACCEPTANCE AND LEBT MATCHING

The RFQ acceptance was determined using an iterative method in TraceWin coupled to the Toutatis library. An initially overfilled beam distribution (50k macroparticles, 30 keV, 4 mA) was tracked through the RFQ, and particles reaching the nominal output energy of 1.5 MeV were identified and mapped to their initial coordinates at the RFQ entrance to reconstruct the accepted phase space. The resulting distribution was used to generate refined input beams, and the procedure was repeated until convergence of the Twiss parameters within 3% was achieved.

For an input emittance of $\varepsilon = 0.15\ \pi\cdot$mm$\cdot$mrad, the matched RFQ entrance parameters were found to be $\alpha = 0.75$ and $\beta = 0.03675$ mm/$\pi\cdot$mrad, yielding a transmission of 99.69%, of which less than 0.02% fail to be accelerated.

Following this, the LEBT line was optimized to match the beam to this RFQ acceptance. The simulations start 60 mm downstream of the ion source extraction aperture, where complex ion source-related effects (e.g., residual magnetic fields, stray electric fields, and space-charge build-up) are assumed negligible.

A uniform transverse distribution of 10k macroparticles was generated at the source with the following parameters:

- $\alpha_{xx'} = \alpha_{yy'} = -5.2571$
- $\beta_{xx'} = \beta_{yy'} = 0.529$ mm/$\pi\cdot$mrad
- $\varepsilon_{xx'} = \varepsilon_{yy'} = 0.12\ \pi\cdot$mm$\cdot$mrad
- Beam energy: 30 keV
- Beam current: 4.017 mA

Space-charge compensation was included up to 95 %, implemented as a gradual reduction of the effective beam current along the LEBT between the ion source and the RFQ entrance.

Matching was achieved by tuning two solenoids using three-dimensional field maps. Due to field asymmetries, additional steering corrections were applied to center the beam in position and angle at the RFQ entrance. This ensured proper phase-space matching and minimized beam losses in the RFQ.

COMPARING TRACEWIN TO DYNAC

A benchmarking study was performed using 1M macro-particles to compare beam dynamics simulations with TraceWin and DYNAC for the combined LEBT and RFQ. In TraceWin, the PICNIR method was used, based on the SCHEFF model with corrections for non-circular beam profiles. A similar SCHEFF approach was used in DYNAC.

In TraceWin, the LEBT was modeled using 3D field maps of the solenoids and integrated steerers. In DYNAC, axisymmetric versions of these fields were used, eliminating the need for steering corrections. The optimized solenoid strengths are listed in Table 1.

Table 1: Peak Solenoid Strengths

	TraceWin	DYNAC
Solenoid 1 (T)	0.16876	0.16920
Solenoid 2 (T)	0.18595	0.18700

The ratios of the solenoid settings differ by 0.3%

The lower plot in Fig. 2 shows the evolution of the 2-σ beam envelope along the LEBT and RFQ for both simulation tools. The larger 4D emittance reported by DYNAC in the beginning of the RFQ in the upper plot is an artifact of it being Z based. Good agreement is observed between both codes, with minor differences attributed to field modeling and space-charge implementation.

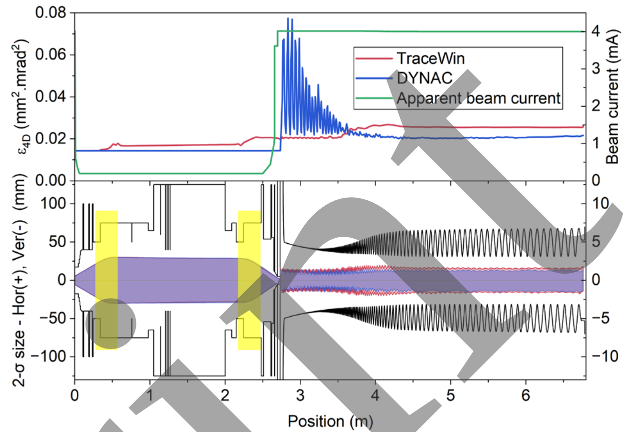

Figure 2: 4D emittance growth through the LEBT and RFQ for TraceWin and DYNAC (SCC implemented via reduced beam current). (lower) Horizontal (+) and vertical (−) beam envelopes; solenoid locations indicated in yellow.

Figure 3 compares the output phase space distributions at the RFQ exit, with corresponding parameters summarized in Table 2.

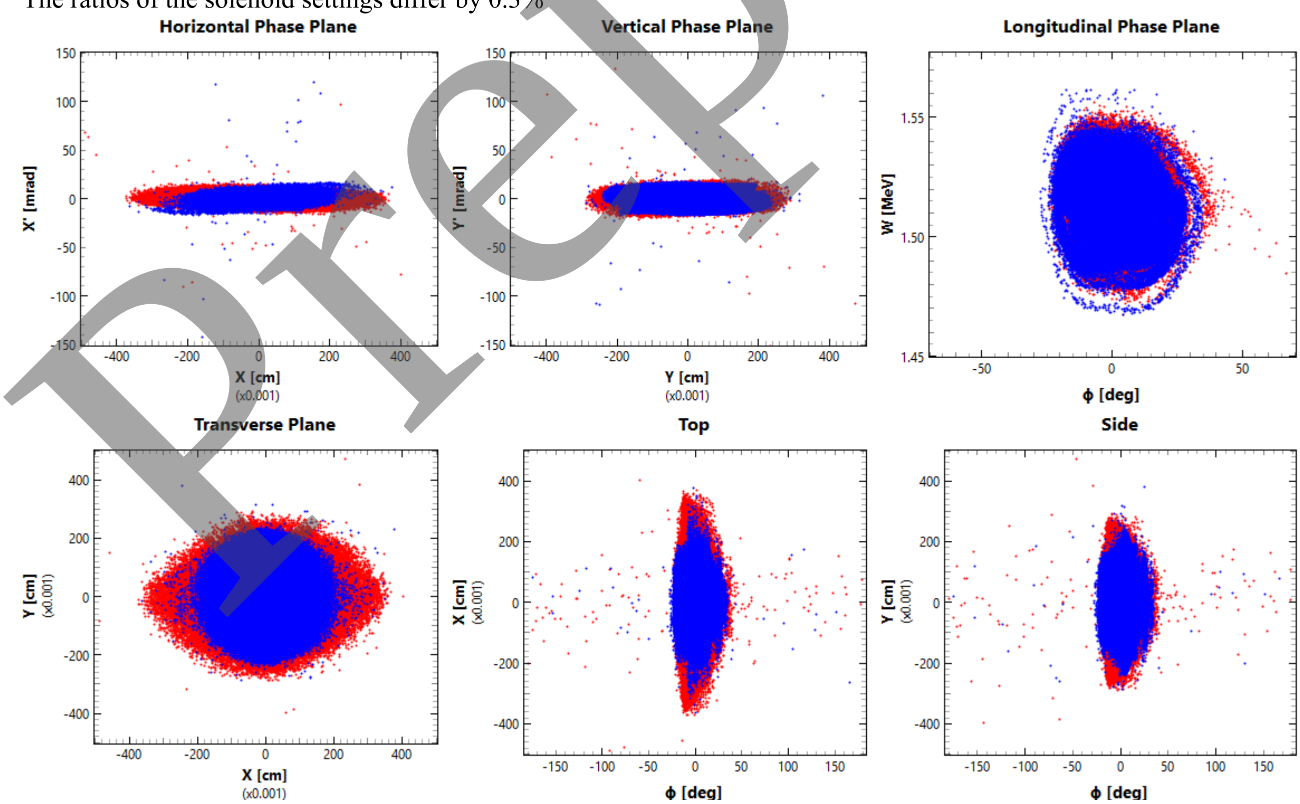

Figure 3: RFQ output phase planes for TraceWin (red) and DYNAC (blue).

Both codes produce similar beam properties, while small differences in halo and fine structure can be linked to differences in numerical methods.

Table 2: Comparison of the Twiss Parameters and Normalized RMS Emittances for the RFQ Output Distributions

	TraceWin	DYNAC
α_x	0.19226	-0.24902
α_y	-0.14028	-0.0811
β_x (mm/π·mrad)	0.27807	0.19404
β_y (mm/π·mrad)	0.17623	0.15044
ε_x (π·mm·mrad)	0.1642	0.1344
ε_y (π·mm·mrad)	0.1620	0.16102
ε_z (π·deg·MeV)	0.09332	0.069455
Beam energy (MeV)	1.5141	1.5107
Transmission (%)	99.69	99.99

ANALYSIS OF RFQ LOSS MECHANISMS

Beam losses in the RFQ were studied using high-statistics TraceWin simulations with 1M macroparticles. Fig. 4 shows the distribution of losses along the RFQ. No significant losses occur in the radial matching and shaping sections (first ~1 m), confirming proper initial matching.

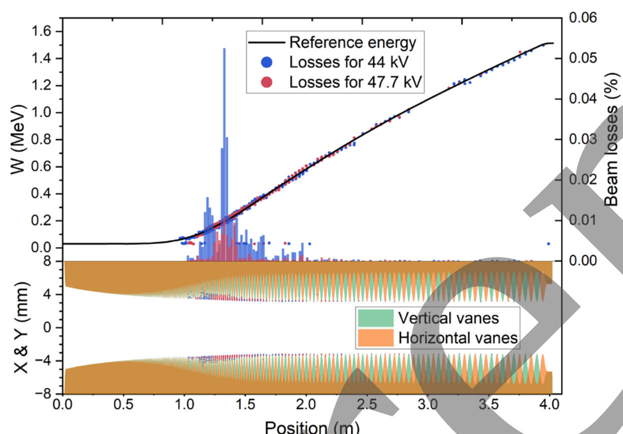

Figure 4: The position of losses in the RFQ displayed at vane voltages of 44 kV (blue) and 47.7 kV (red). Individual lost particles are displayed at the energy at which they are lost. (lower) The vane profiles and the coordinates of lost particles as they get intercepted.

Most losses arise during the gentle bunching and early acceleration phases, where particles outside the longitudinal acceptance drift out of phase and are subsequently lost on the vane tips. While some particles are initially captured, a fraction is lost at higher energies. The majority of losses occur below 0.8 MeV, indicating that longitudinal capture is the dominant limitation.

To further investigate performance margins, simulations were performed at an increased vane voltage of 47.7 kV, compared to the nominal 44 kV. This resulted in a reduction of beam losses, increasing the transmission from 99.69% to 99.91%.

In addition to improved transmission, a noticeably cleaner longitudinal phase space distribution was obtained at higher vane voltage (see Fig. 5). The spread in phase is significantly reduced. This suggests enhanced longitudinal focusing and more robust bucket confinement, but practical limitations such as RF power and breakdown thresholds must be considered during operation.

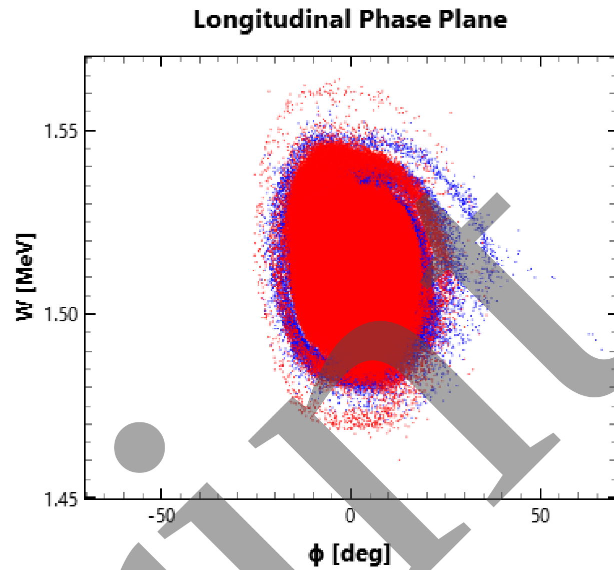

Figure 5: Longitudinal phase plane at the RFQ exit for a vane voltage of 44 kV (blue) and 47.7 kV (red).

However, early simulations indicate that the extended spread in energy might induce additional losses further down the accelerator.

CONCLUSION

The MYRRHA Phase 1 injector front-end has been studied with a focus on LEBT matching and RFQ performance. The RFQ acceptance was determined using an iterative backtracking method, resulting in a transmission of 99.69% for an input emittance of 0.15 π·mm·mrad. The LEBT was successfully matched under 95% space-charge compensation using field maps.

Although good agreement is found between TraceWin and DYNAC in beam transport and output distributions, some further studies are ongoing to better understand the small differences observed. RFQ losses are dominated by incomplete longitudinal capture below 0.8 MeV. Increasing the vane voltage to 47.7 kV improves transmission to 99.91% and reduces phase spread.

These results demonstrate that the injector front-end design meets performance requirements.

REFERENCES

[1] TraceWin code, `https://www.dacm-logiciels.fr/`

[2] DYNAC code, `https://github.com/dynac-source`

[3] H. Aït Abderrahim et al., "MYRRHA Accelerator Experiment, Research and Development Programme," *CORDIS*, Project ID: 662186.

[4] F. Bouly, "MYRRHA start-to-end design studies," IN2P3, Grenoble, France, 2020.

[5] K.R. Crandall, R.H. Stokes, and T.P. Wangler, in *Proc. LINAC'79*, Montauk, NY, USA, 1979, pp. 205–210.